Cellular and Molecular Life Sciences (2023) 80:315
https://doi.org/10.1007/s00018-023-04965-8

ORIGINAL ARTICLE

BCAT2 promotes melanoma progression by activating lipogenesis via the epigenetic regulation of FASN and ACLY expressions

Yangzi Tian[1] · Jingjing Ma[1] · Hao Wang[1] · Xiuli Yi[1] · Huina Wang[1] · Hengxiang Zhang[1] · Sen Guo[1] · Yuqi Yang[1] · Baolu Zhang[1] · Juan Du[1] · Qiong Shi[1] · Tianwen Gao[1] · Weinan Guo[1] · Chunying Li[1]

Received: 30 December 2022 / Revised: 17 August 2023 / Accepted: 13 September 2023 / Published online: 6 October 2023

Abstract

Melanoma is the most lethal skin cancer originating from the malignant transformation of epidermal melanocyte. The dysregulation of cellular metabolism is a hallmark of cancer, including in melanoma. Aberrant branched-chain amino acids (BCAA) metabolism and related enzymes has been greatly implicated in the progression of multiple types of cancer, whereas remains far from understood in melanoma. Herein, we reported that the critical BCAA metabolism enzyme branched-chain amino acid transaminase 2 (BCAT2) is an oncogenic factor in melanoma by activating lipogenesis via the epigenetic regulation of fatty acid synthase (FASN) and ATP-citrate lyase (ACLY) expressions. Firstly, we found that BCAT2 expression was prominently increased in melanoma, and highly associated with clinical stage. Then, it was proved that the deficiency of BCAT2 led to impaired tumor cell proliferation, invasion and migration in vitro, and tumor growth and metastasis in vivo. Further, RNA sequencing technology and a panel of biochemical assays demonstrated that BCAT2 regulated de novo lipogenesis via the regulation of the expressions of both FASN and ACLY. Mechanistically, the inhibition of BCAT2 suppressed the generation of intracellular acetyl-CoA, mitigating P300-dependent histone acetylation at the promoter of *FASN* and *ACLY*, and thereby their transcription. Ultimately, zinc finger E-box binding homeobox 1 (ZEB1) was identified as the upstream transcriptional factor responsible for BCAT2 up-regulation in melanoma. Our results demonstrate that BCAT2 promotes melanoma progression by epigenetically regulating FASN and ACLY expressions via P300-dependent histone acetylation. Targeting BCAT2 could be exploited as a promising strategy to restrain tumor progression in melanoma.

Keywords BCAT2 · FASN · ACLY · Lipogenesis · Melanoma · Epigenetic

Abbreviations

ACAT2	Acetyl-CoA acetyltransferase 2
Ac-H3	Acetyl-Histone H3
ACLY	ATP-citrate lyase
BCAAs	Branched-chain amino acids
BCAT2	Branched-chain amino acid transaminase 2
BCKA	Branched-chain keto acid
BCKDH	Branched-chain alpha-keto acid dehydrogenase complex
CCK8	Cell Counting Kit-8 assay
ChIP	Chromatin immunoprecipitation
DBT	Dihydrolipoamide branched chain transacylase E2
EMT	Epithelial-to-mesenchymal transition
FASN	Fatty acid synthase
FFA	Free fatty acids
GSEA	Gene set enrichment analysis
HMGCR	3-Hydroxy-3-methylglutaryl-CoA
NaAc	Sodium acetate
NHEM	Normal human epidermal melanocyte
PA	Palmitic acid
PDAC	Pancreatic ductal adenocarcinoma
SCD	Stearoyl-CoA desaturase
SSO	Sulfosuccinimidyl oleate sodium
TMA	Tumor tissue microarrays
ZEB1	Zinc finger E-box binding homeobox 1
αKG	α-Ketoglutarate

Yangzi Tian, Jingjing Ma and Hao Wang contributed equally.

✉ Weinan Guo
guown@fmmu.edu.cn

✉ Chunying Li
lichying@fmmu.edu.cn

[1] Department of Dermatology, Xijing Hospital, Fourth Military Medical University, Xi'an, Shaanxi, China

Introduction

Melanoma is the most lethal skin cancer originating from the malignant transformation of epidermal melanocyte [1]. While melanomas at early stage can be easily cured by early surgical resection, metastatic melanoma are difficult to treat due to resistance to current available therapies and the inevitable occurrence of relapse [2]. The progress of targeted therapy and immunotherapy has brought revolutionary advances in improving the prognosis of patients. Nevertheless, low response rate and treatment resistance significantly hinder therapeutic efficacy [3]. Therefore, it is of necessity to forwardly elucidate the mechanism underlying melanoma pathogenesis and develop more therapeutic options.

The dysregulation of cellular metabolism is a hallmark of cancer. Multiple paradigms of cellular metabolism like glycolysis, lipid metabolism and amino acid metabolism have been reported to not only mediate the malignant behavior of tumor cells, but also regulate the tumor-infiltrating immune cells [4]. BCAAs that comprise of leucine, isoleucine, and valine are the most hydrophobic and essential amino acids for protein synthesis and molecular signals [5]. Branched-chain amino acid transaminase 1 and 2 (BCAT1/2) transfers nitrogen of BCAAs to α-ketoglutarate (αKG) to produce glutamine and branched-chain keto acid (BCKA), which is then metabolized by branched-chain alpha-keto acid dehydrogenase complex (BCKDH) to produce tricarboxylic acid (TCA) cycle intermediates acetyl-CoA and/or succinyl-CoA for energy production and macromolecules biogenesis [6]. As is similar to other types of cancers, BCAT1 expression is prominently increased in melanoma, and the knockdown of BCAT1 restrains melanoma progression [7]. In addition, melanoma cells harboring *BRAF* mutation are highly relied on leucine for survival. What's more, genome-wide CRISPR/Cas9 knockout screening identified that dihydrolipoamide branched-chain transacylase (DBT), a subunit of BCKDH, regulated cell apoptosis induced by $BRAF^{V600E}$ overexpression in melanocytes, acting as a gatekeeper in mutant *BRAF*-driven melanocyte malignant transformation [8]. Recently, the role of BCAT2 in cancer pathogenesis has been revealed mainly in pancreatic cancer. The pancreatic tissue-specific knockout of *Bcat2* significantly impeded the progression of tumor, and a lower-BCAA diet also impeded pancreatic ductal adenocarcinoma (PDAC) development in mice. [9]. In response to BCAA deprivation, the acetylation of BCAT2 led to its degradation and thereby ameliorated cell proliferation and pancreatic tumor growth [10]. In contrast, a high-BCAA diet promoted PDAC development by USP1-mediated BCAT2 stabilization [11]. While these reports have shed some lights on the role of BCAT2 in pancreatic tumor, the role of BCAT2 in melanoma remain elusive.

Herein, we firstly found that BCAT2 expression was significantly increased in melanoma compared with normal human melanocyte and nevus, respectively. Then, through either genetic or pharmacological intervention, the role of BCAT2 in melanoma progression was revealed both in vitro and in vivo. Subsequently, RNA sequencing and a panel of biochemical assays were employed to demonstrate the underlying mechanism. Ultimately, the upstream regulatory mechanism of BCAT2 up-regulation was also revealed.

Materials and methods

Further information is supplied in Supplementary Materials and Methods

Transwell assay

Migration assay were applied using 24-well inserts with an 8 μm pore size (Corning, NY). In brief, a total of 500 μl DMEM medium containing 10% fetal bovine serum (FBS) was added to the lower part of each transwell chamber, and 200 μl DMEM medium without FBS containing 2×10^4 cells was added to the upper part. After 24 h, the cells that had migrated under the membrane were fixed and then stained with crystal violet. For measuring cell invasion, similar steps were followed, but the transwell chambers used were coated with Matrigel (BD Biosciences, NJ). The motile or invasive cells were stained with crystal violet. To quantify invading and migrating cells, stained cells were counted using the "Multi-point" tool in ImageJ software (NIH). Five fields per well (Olympus, Tokyo, Japan) were counted under an inverted system microscope.

Cell viability assay

Cell viability was analyzed by the Cell Counting Kit-8 assay (SeaBioTech, Shanghai, China). Cells were seeded in 96-well plates at a density of 5000 cells per well, with each well containing 200 μl of complete culture medium. The plates were then incubated at 37℃ for 24, 48, 72 and 96 h respectively. Then culture medium was discarded and replaced with 100 μl of Cell Counting Kit-8 working solution (0.05 μg/μl Cell Counting Kit-8 (0.5 mg/ml) reagent) and cells were incubated at 37 °C. After 0.5-1 h, the absorbance of the culture medium was detected at 450 nm with a micro-plate reader (Bio-Rad, Hercules, CA).

Colony formation assay

To evaluate long-term cell survival, a colony formation assay was conducted using melanoma cells subjected to the indicated treatment. After treatment, cells were digested and re-seeded with the number of 3,000 cells per well into a 6-well plate (in triplicate). The re-seeded cells were allowed to adhere and grow for a duration of 14 days. The cells were fixed with 4% paraformaldehyde for 15 min and visualized by 0.5% (w/v) crystal violet (Sigma Aldrich, St. Louis, USA) staining. The numbers of colonies were quantified using the ImageJ software. Representative images were captured from at least nine similar wells, chosen from three independent experiments.

RNA isolation and qRT-PCR

Total RNA was extracted by the TRIzol reagent (cat.15596018, Invitrogen, Carlsbad, CA, USA). mRNA was reverse-transcribed to cDNA employing the PrimeScriptTM RT Master Mix kit (cat. RR036A, TaKaRa, Tokyo, Japan), and qRT-PCRs were carried out employing the SYBR Premix Ex TaqTM II kit (cat. RR820A, TaKaRa, Tokyo, Japan) and performed with a multicolor real-time PCR detection system (iQTM5, Bio-Rad, Hercules, CA, USA). Primers used in the study were listed in Supplementary Table S1. The relative gene expression levels were all normalized to β-actin mRNA and calculated using the $2^{-\Delta\Delta CT}$ method.

Lentiviral vectors, plasmid vectors, and siRNA transfection

To obtain the suppression of BCAT2 expression, melanoma cells were infected with a lentiviral vector encoding a specific short hairpin RNA (shRNA) against *BCAT2* according to the manufacturer's protocol. After 72 h of transfection, null cells were removed with puromycin to obtain stably infected clones. Lentiviral vectors were from GenePharma, Shanghai, China. Knockdown of BCAT2 in A375 and A2058 melanoma cells using small interfering RNA and lipofectamine 3000 transfection reagent kit (L3000-015, Invitrogen, Carlsbad, CA). For BCAT2 overexpression, the expression plasmid BCAT2 and the empty plasmid con468 (pcdna3.1-cmv-mcs-3flag-ef1a-zsgreen-sv40-purromycin) were designed and synthesized in Genechem, Shanghai, China. For ZEB1 overexpression, ZEB1 overexpression plasmid (PEGFP-N1-CMV enhancer-CMV promoter-C-EGFP-SV40 poly(A)) was designed and synthesized by Tsingke Biotechnology Co., Ltd., in Beijing. The sequences of shRNA against *BCAT2* and the siRNA sequences against *BCAT2* and *ZEB1* are shown in Supplementary Table S2.

RNA-sequencing analysis

Total RNA extraction was performed using Trizol reagent from A2058 cells that had received the indicated treatment. Following RNA extraction, the RNA samples were processed and analyzed using RNA sequencing (RNA-seq) by Gene Denovo Biotechnology Co., Ltd (Guangzhou, China). The RNA-seq data used in this study have been deposited in the National Center for Biotechnology Information's Sequence Read Archive (Sequence Read Archive study accession code PRJNA911770; https://www.ncbi.nlm.nih.gov/sra/PRJNA911770).

Chromatin Immunoprecipitation (ChIP) assay and ChIP-sequencing

ChIP assay was performed with lysates prepared from melanoma cells after indicated treatment and then measured by the SimpleChIP Plus Sonication Chromatin IP Kit (#56383, CST, Danvers, MA, USA) following the manufacturer's instructions. In short, immunoprecipitation was performed with primary antibody as well as an isotype control IgG antibody (Antibodies used for ChIP were described in Reagents and Antibodies part). RNase A and proteinase K treated immunoprecipitated DNA and starting DNA from aliquots of cell lysates were purified by phenol–chloroform extraction and ethanol precipitation. Purified and genomic DNA were analyzed by RT-PCR. Supplementary Table S1 depicts the primer sequences used in this research. % of Input was calculated by using $100\% \times 2^{(-\Delta CT)}$, and $\Delta CT = Ct\ (Ip) - Ct\ (Input)$.

ChIP-sequencing was employed to examine the enrichment of histone acetylation on the promoter regions of *FASN* and *ACLY* genes in A2058 murine tumor samples obtained from nude mice receiving BCAA dietary intervention. Briefly, tumor tissues isolated from nude mice receiving different BCAA diet groups were cut into pieces of 1 mm^3, and all tissues were then immediately placed in liquid nitrogen and preserved at − 80 °C. After that, all the samples were sent to the Seqhealth Technology Co., Ltd. (Wuhan, China) for library preparation and sequencing. The data of ChIP-sequencing has been submitted to the NCBI Gene Expression Omnibus (GEO) database with the accession number GSE 240663.

hTF (Transcription factor) target analysis

Promoter region sequences for human BCAT2 was obtained via https://www.ncbi.nlm.nih.gov/gene/. The binding sites for transcription factor ZEB1 to BCAT2 promoter, Ac-H3 to ACLY promoter and FASN promoter were predicted by JASPAR databases. According to the predicted scores, the higher scoring binding sites were chosen for validation by

chromatin-immunoprecipitation (ChIP) assay, and the most significantly enriched sites were used for real time PCR analysis.

Cell lines and reagents

Details for cell lines and reagents are described in Supplementary Materials and Methods.

Western blotting analysis

Details for western blotting are described in Supplementary Materials and Methods.

Immunofluorescence staining analysis

Details for immunofluorescence staining are provided in Supplementary Materials and Methods.

Immunohistochemistry staining analysis

Details for immunohistochemical staining are provided in Supplementary Materials and Methods.

Acetyl-CoA and free fatty acid quantification

Details for acetyl-CoA and free fatty acid quantification are provided in Supplementary Materials and Methods.

Oil red O staining

Details for oil red O staining are provided in Supplementary Materials and Methods.

Flow cytometry analysis of cell apoptosis

Details for flow cytometry analysis of cell apoptosis are provided in Supplementary Materials and Methods.

In vivo study

Details for animal experiments are provided in Supplementary Materials and Methods.

Statistical analysis

All data represent the mean ± SD (standard deviation) from at least three independent experiments. Two-group comparisons were using two-tailed Student unpaired t test. Spearman's rank correlation coefficient analysis was used to calculate the correlation between the staining scores of different molecules in TMA. All statistical analyses were performed with GraphPad Prism 8.0, and P value < 0.05 (*) was considered statistically significant.

Results

BCAT2 expression is significantly increased in melanoma

We firstly examined the expression status of BCAT2 in melanoma. Through qRT-PCR and immunoblotting analysis, either the mRNA or protein level of BCAT2 was prominently increased in melanoma, compared with normal human epidermal melanocyte (NHEM) and immortalized melanocyte cell line PIG1, respectively (Fig. 1a, b). Immunofluorescence staining analysis showed that BCAT2 was mainly localized to cytoplasm in melanoma cells (Fig. 1c). In addition, the staining intensity of BCAT2 was higher in both primary and metastatic melanoma tissues compared with that in nevus (Fig. 1d), and exerted a trend of increase in metastatic melanoma tissues compared with that in primary melanoma tissues (Fig. 1d). Further, immunohistochemical staining analysis in TMA displayed that BCAT2 expression was prominently increased in melanoma compared to that in nevus, and was higher in metastatic melanoma tissues than that in primary ones (Fig. 1e). Of note, the expression of BCAT2 displayed a trend of increase as the T stage progressed (Fig. 1f). Therefore, BCAT2 expression is significantly increased in melanoma, indicating its potential oncogenic role.

BCAT2 acts as an oncogenic factor in melanoma

In order to testify the role of BCAT2 in melanoma pathogenesis, three independent siRNAs against *BCAT2* were established to obtain the knockdown of BCAT2 (Fig. 2a), and the first two siRNAs were chosen to perform the following experiments. The CCK8 assay revealed that BCAT2 deficiency had minimal impact on cell viability in a relatively shorter duration (within 96 h) (Fig. 2b). In consistent, BCAT2 expression deficiency minimally triggered cell death (Fig. 2c). However, BCAT2 deficiency induced prominent suppression of colony formation in a relatively longer term (14 days), with the relative proliferation rate decreasing from 100% in control group to around 50–70% (Fig. 2d), suggesting that BCAT2 is required for long-term melanoma cell proliferation. More than this, transwell assay and wound healing assay showed that BCAT2 expression deficiency led to prominent impairment of melanoma cell invasion and migration (Fig. 2e, f). Besides, pharmacological inhibition of BCAT2 via BCAT-IN-2 treatment effectively suppressed the formation of melanoma cell colony, with the relative proliferation rate

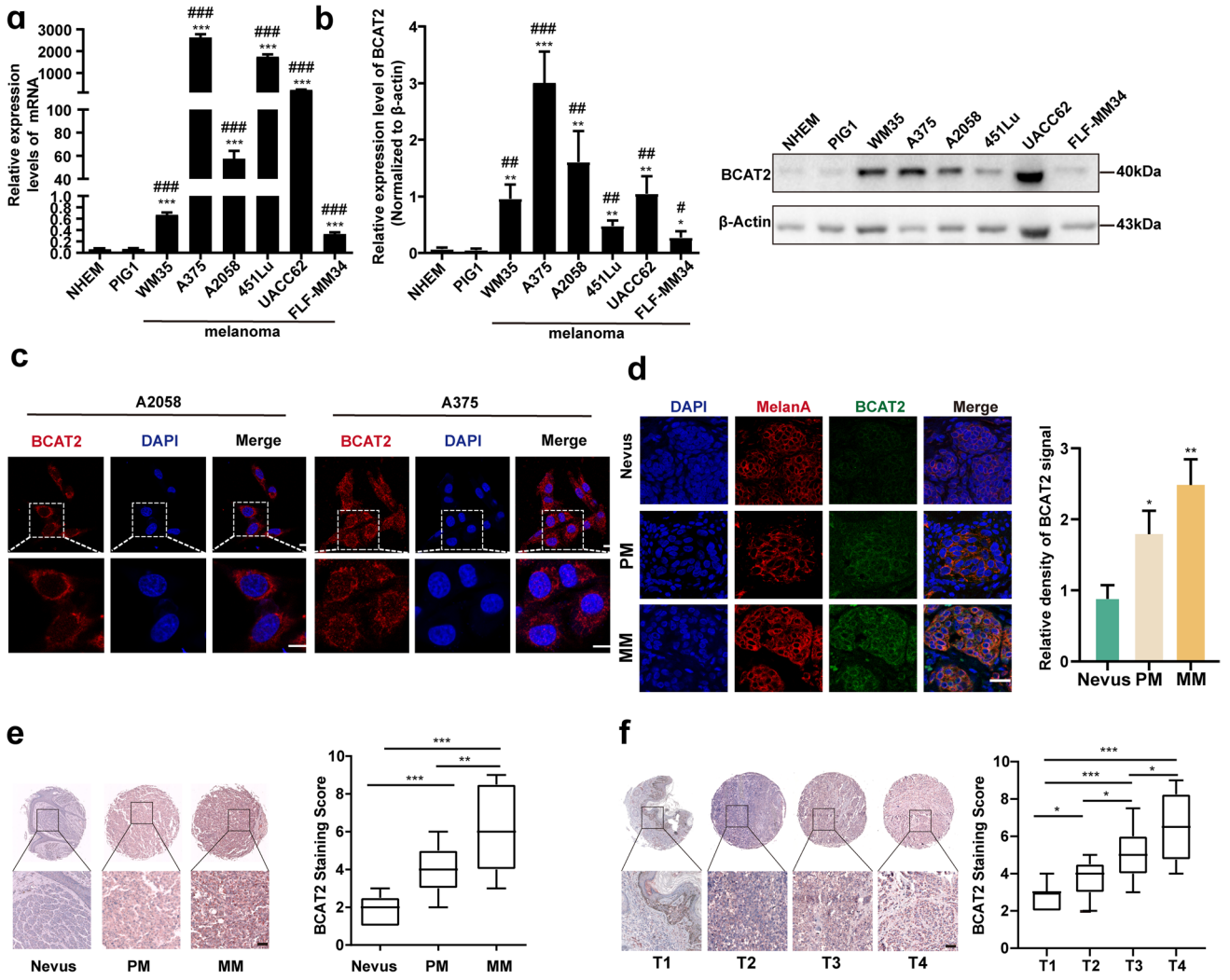

Fig. 1 BCAT2 expression is significantly increased in melanoma. **a-b** Relative mRNA and protein levels of BCAT2 in NHEM, PIG1 and a panel of melanoma cell lines. **c** Immunofluorescence staining analysis of intracellular BCAT2 distribution in both A2058 and A375 melanoma cell lines. Scale bar = 10 μm. **d** Immunofluorescence staining analysis of BCAT2 expression in nevus tissues and melanoma tissues. Scale bar = 50 μm. **e** Immunohistochemical staining analysis of BCAT2 in melanoma TMA. Scale bar = 50 μm. **f** The staining scores of BCAT2 in melanoma tissues in TMA at different T stages. Scale bar = 50 μm. Data represent the mean ± SD of triplicates. *P* value was calculated by two tailed Student's t-test, $^{*}P<0.05$, $^{**}P<0.01$, $^{***}P<0.001$, NHEM group as control; $^{\#}P<0.05$, $^{\#\#}P<0.01$, $^{\#\#\#}P<0.001$, PIG1 group as control. ns, non-significant

reducing from 100% to around 50%, so were the invasion and migration of melanoma cells (Fig. 2g, h). To avoid the off-target effect, we performed rescue experiment via the employment of the overexpression of BCAT2 in melanoma cells with the knockdown of BCAT2 in both A2058 and A375 melanoma cell lines (Supplementary Fig. 1a). As was revealed, the overexpression of BCAT2 prominently reversed the impairment of colony formation in melanoma cells with BCAT2 deficiency in both A2058 and A375 cell lines (Supplementary Fig. 1b). In addition, BCAT2 overexpression could also almost fully reverse the reduction of tumor cell invasion and migration resulted by the knockdown of BCAT2 (Supplementary Fig. 1c, d). Taken together, BCAT2 plays an oncogenic role in melanoma in vitro.

Pre-clinical mice model was established to forwardly confirm the oncogenic effect of BCAT2 on melanoma pathogenesis in vivo (Fig. 3a). The knockdown of BCAT2 led to prominent regression of tumor, as revealed by the reduction of tumor volumes and tumor weights (Fig. 3b–d). In addition, nude mice burdened with A2058 melanoma cells were supplied with normal diet or low-BCAA diet or high-BCAA diet to see the effect of BCAA supplement on tumor growth (Fig. 3e). The concentration of BCAA in blood was examined in each group, and the result confirmed that high-BCAA diet efficiently induced the up-regulation of

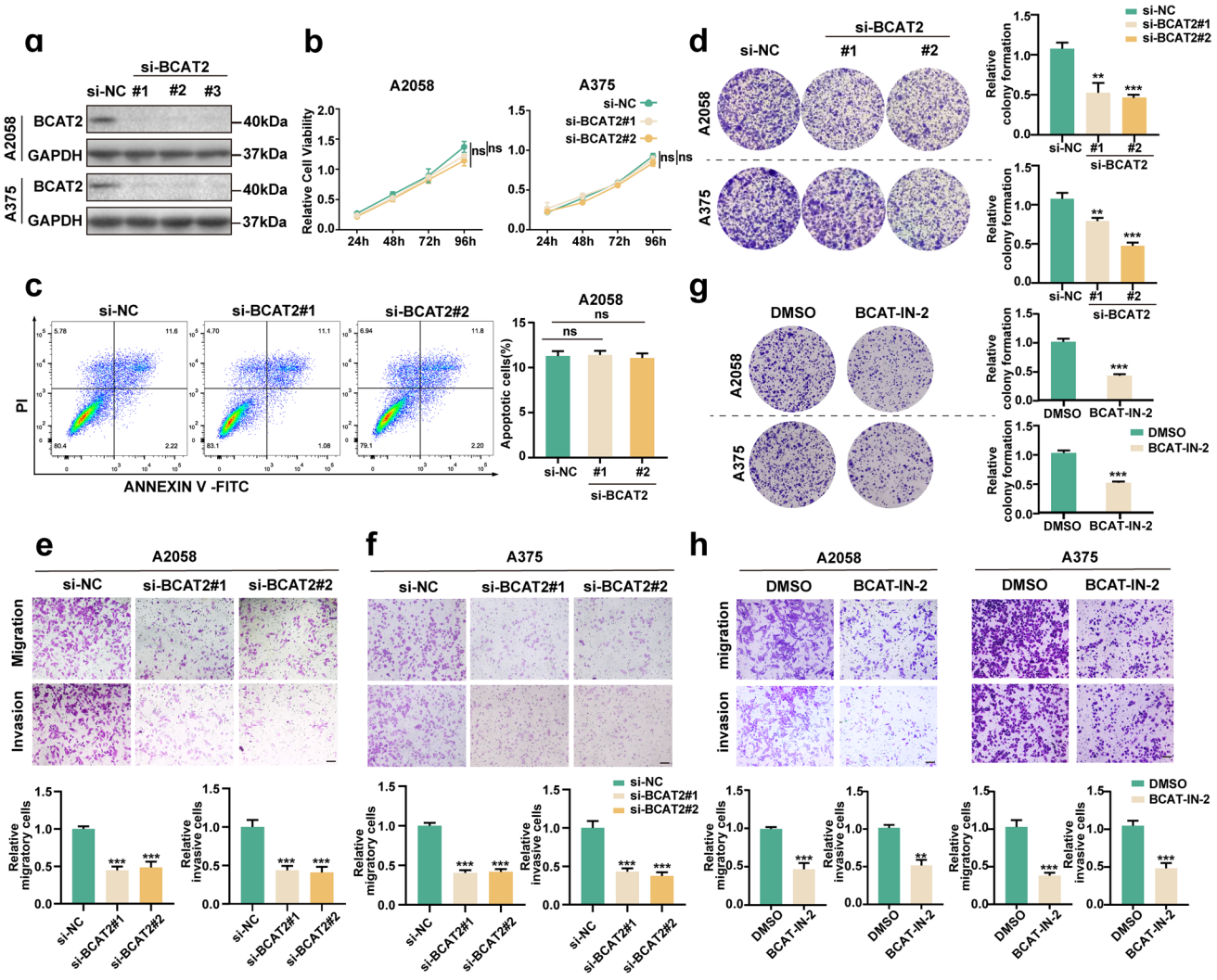

Fig. 2 BCAT2 promotes melanoma cell proliferation, invasion and migration. **a** The knockdown efficiency of BCAT2 in both A2058 and A375 melanoma cell lines. **b** Relative cell viability of A2058 and A375 melanoma cell lines after the intervention of BCAT2. **c** Flow cytometry analysis of cell apoptosis in A2058 cells after the knockdown of BCAT2. **d** Relative colony formation of melanoma cells in both A2058 and A375 melanoma cells after the knockdown of BCAT2. **e–f** Tumor cell migration and invasion in both A2058 and A375 melanoma cells after the knockdown of BCAT2. Scale bar = 100 μm. **g** Relative colony formation of melanoma cells in both A2058 and A375 melanoma cells treated with BCAT2 inhibitor (BCAT-IN-2, 80 μM). **h** Tumor cell migration and invasion in both A2058 and A375 melanoma cells after the pharmacological inhibition of BCAT2 (BCAT-IN-2, 80 μM). Scale bar = 100 μm. PM, primary melanoma; MM, metastatic melanoma. Data represent the mean ± SD of triplicates. *P* value was calculated by two tailed Student's t-test, $^{**}P < 0.01$, $^{***}P < 0.001$, ns, non-significant

circulating BCAA level, whereas low-BCAA diet resulted in down-regulation of circulating BCAA level (Supplementary Fig. 1e). As expected, high-BCAA diet significantly promoted the growth of tumor, whereas low-BCAA diet prominently delayed the growth of tumor (Fig. 3f, h). Additionally, the pro-metastatic role of BCAT2 was also examined in vivo in C57BL/6 tumor metastasis mice model (Fig. 3i). Mouse receiving the injection of melanoma cells with the knockdown of BCAT2 exhibited diminished number of lung metastasis (Fig. 3j–l). Concurrent immunofluorescence staining analysis showed that BCAT2 deficiency prominently induced Ki-67 down-regulation in implanted tumor (Fig. 3m, n). In addition, the pro-metastatic role of BCAT2 was proved by diminished immunofluorescence staining intensity of Melan-A (melanoma cell marker) in lung (Fig. 3o). In order to avoid the off-target effect of shRNA in vivo, tumor cells with the knockdown of BCAT2 were stably overexpressed with BCAT2 and then subcutaneously injected into the flank of the nude mice (Supplementary Fig. 1f). As was revealed, the overexpression of BCAT2 could almost fully reverse the suppressive role of BCAT2 knockdown on tumor growth, reflected by either

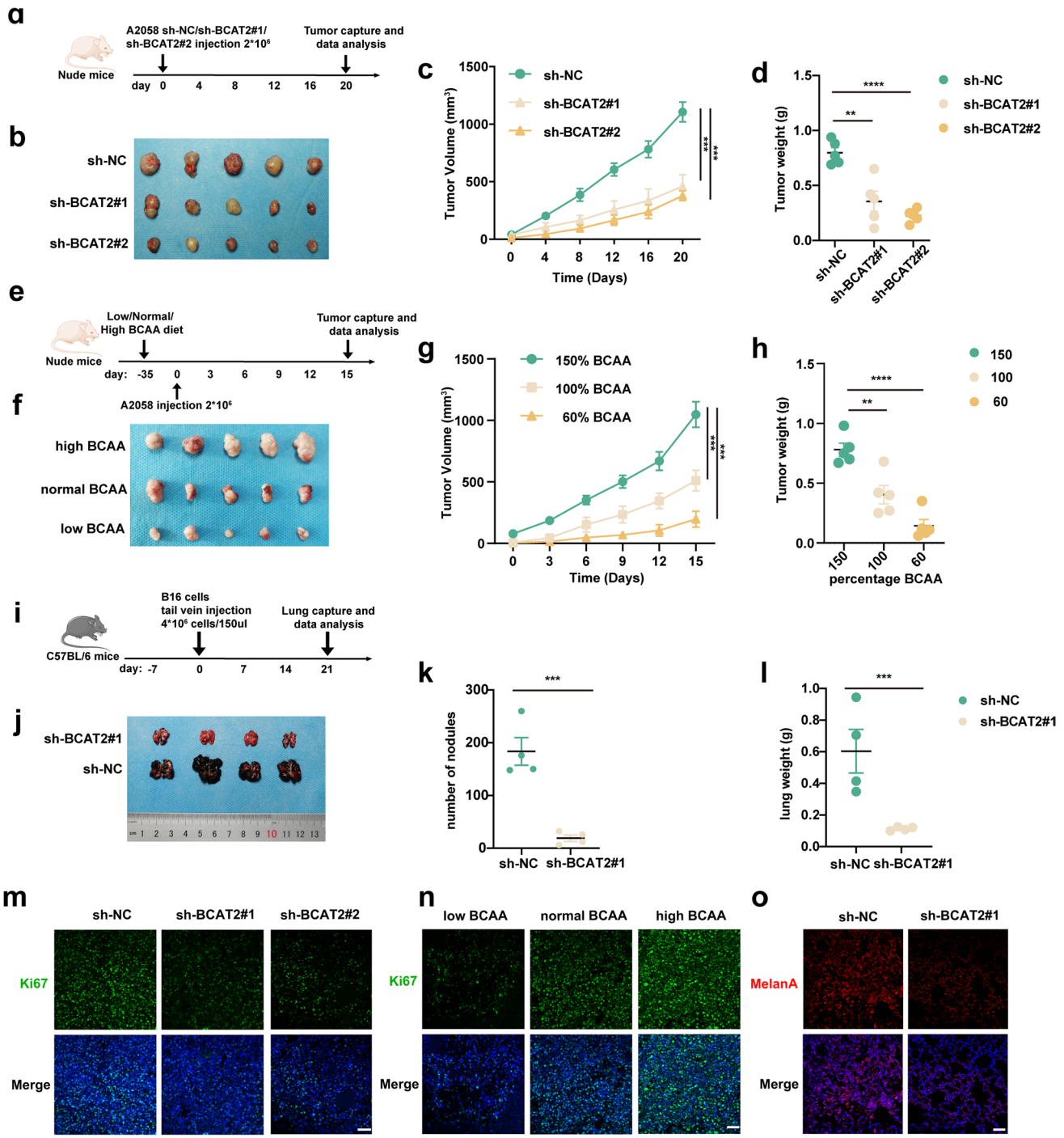

Fig. 3 BCAT2 promotes tumor growth and metastasis in melanoma. **a** A schematic view of the transplantation plan that nude mice burdened with sh-NC or sh-BCAT2#1 or sh-BCAT2#2-transfected A2058 tumors. **b-d** Images of A2058 xenografts with indicated transfection isolated from mice. Tumor volumes and weights in each group were calculated and displayed on the right. Symbols of one dot indicates one mouse. **e** A schematic view of the treatment plan that nude mice burdened with A2058 tumors. **f–h** Images of A2058 xenografts isolated from mice receiving indicated diet. Tumor volumes and weights in each group were calculated and displayed on the right. Symbols of one dot indicates one mouse. **i** A schematic view of the establishment of tumor metastasis model via caudal vein injection of B16 cells into C57BL/6 mice. **j-l** Images of lungs isolated from mice in indicated group. The number of modules and lung weight in each group were calculated and displayed on the right. Symbols of one dot indicates one mouse. **m–n** Immunofluorescence staining analysis of Ki-67 in isolated tumors with indicated interventions. Scale bar = 50 μm. **o** Immunofluorescence staining analysis of MelanA in lung isolated from mice in indicated groups. Scale bar = 50 μm. Data represent the mean ± SD of triplicates. *P* value was calculated by two tailed Student's t-test, $^{**}P < 0.01$, $^{***}P < 0.001$, $^{****}P < 0.0001$

tumor volume or tumor weight (Supplementary Fig. 1 g–i). What's more, murine B16 melanoma cells with the deficiency of BCAT2 were also stably overexpressed with BCAT2, and then subcutaneously injected into the tail of the C57BL/6 mice (Supplementary Fig. 1j). Similarly, the overexpression of BCAT2 could largely reverse the suppressive role of BCAT2 deficiency on tumor metastasis in lung (Supplementary Fig. 1 k-m). Taken together, BCAT2 up-regulation significantly contributes to melanoma growth and metastasis in vivo.

BCAT2 up-regulation activates lipogenic pathway in melanoma

Thereafter, RNA-sequencing technology was employed to see the downstream molecules regulated by BCAT2. There were in total 140 molecules displaying more than twofold change in BCAT2-knockdown group compared with control group (Fig. 4a). Gene set enrichment analysis (GSEA) showed that the differentially-expressed molecules between BCAT2-knockdown group and control group were enriched in multiple biological pathways, including de novo lipogenesis (Fig. 4b, c). Several critical enzymes greatly implicated in lipid metabolism including ATP-citrate lyase (ACLY), acetyl-CoA acetyltransferase 2 (ACAT2), fatty acid synthase (FASN), 3-hydroxy-3-methylglutaryl-CoA (HMGCR) and stearoyl-CoA desaturase (SCD) were significantly reduced in BCAT2-knockdown group according to the results of RNA sequencing (Fig. 4d). Further qRT-PCR analysis verification showed that BCAT2 deficiency induced prominent reduction FASN and ACLY mRNA levels, whereas ACAT2, HMGCR and SCD were not prominently altered, in both A2058 and A375 melanoma cells (Fig. 4e & Supplementary Fig. 2a). Concurrent immunoblotting analysis revealed the consistent results (Fig. 4f and Supplementary Fig. 2b). Besides, BCAT-IN-2 treatment also induced the suppression of both FASN and ACLY expressions (Fig. 4g and Supplementary Fig. 2c). Oil red staining showed that the pharmacological inhibition of BCAT2 led to reduced content of intracellular lipid in both A2058 and A375 melanoma cells (Fig. 4h and Supplementary Fig. 2d). Forward free lipid acid detection displayed that BCAT-IN-2 treatment led to prominent reduction of intracellular palmitic acid in both A2058 and A375 melanoma cells, indicating that BCAT2 promoted lipogenesis in melanoma cells (Fig. 4i and Supplementary Fig. 2e). Additionally, the analysis in TCGA SKCM database displayed that BCAT2 was in significant correlation with either FASN or ACLY mRNA level (Fig. 4j). The staining intensity of BCAT2 was also significantly correlated with that of either FASN or ACLY in TMA (Fig. 4k). Of note, to avoid the off-target effect of siRNA against *BCAT2*, melanoma cells with the knockdown of BCAT2 were overexpressed with BCAT2, in order to confirm the impact of BCAT2 on the expressions of FASN and ACLY. The reduction of FASN and ACLY expressions after the knockdown of BCAT2 could be prominently rescued by the overexpression of BCAT2, both in mRNA and protein levels, in A2058 melanoma cell (Supplementary Fig. 2f). Taken together, BCAT2 regulates the expressions of FASN and ACLY to facilitate lipogenesis in melanoma.

We forwardly proved that whether the oncogenic role of BCAT2 in melanoma was dependent on FASN/ACLY-dependent lipogenic effect. Free lipid acid detection assay revealed that either FASN or ACLY inhibition could reverse the pro-lipogenic effect of BCAT2 (Fig. 5a). The combined inhibition of both forwardly induced the reduction of intracellular free lipid content (Fig. 5a). Oil red staining also showed that while BCAT2 promoted lipid generation, FASN/ACLY inhibitor or the combination would reverse the alteration trend in both A2058 and A375 melanoma cells (Fig. 5b and Supplementary Fig. 2 g). While BCAT2 overexpression increased the number of melanoma cell colonies, concurrent FASN/ACLY inhibition could attenuate the facilitative role of BCAT2, and the combined inhibition of both induced more suppression of colony formation in both A2058 and A375 melanoma cells (Fig. 5c and Supplementary Fig. 2 h). What's more, the inhibition of either FASN/ACLY significantly suppressed the effect of BCAT2 on melanoma cell invasion and migration, and the combined inhibition led to more prominent effect in both melanoma cell liens (Fig. 5d and Supplementary Fig. 2i). In order to forwardly confirm that the oncogenic effect of BCAT2 was associated with fatty acid, we went to see whether the intervention of lipid supply would affect the phenotype associated with BCAT2 knockdown. As a result, while the mono-treatment with CD36 (fatty acid transporter) inhibitor (sulfosuccinimidyl oleate sodium, SSO) induced minimal cell death of melanoma cells compared with control, it prominently potentiated cell death of melanoma cells with the deficiency of BCAT2 (Supplementary Fig. 3a). In addition, the supply of palmitic acid in culture medium could partially reverse the impairment of colony formation, tumor cell invasion and migration induced by the knockdown of BCAT2 in both A2058 and A375 melanoma cells (Supplementary Fig. 3b-c). Therefore, the tumorigenic role of BCAT2 was dependent on lipogenesis activation via the up-regulation of ACLY and FASN expressions.

BCAT2 epigenetically regulates FASN and ACLY expressions via P300-dependent histone acetylation

Since that BCAT2 is responsible for BCAA catabolism that promotes the generation of acetyl-CoA [9], and the increased acetyl-CoA facilitates histone acetylation and thereby the transcriptional of some downstream genes [12], we proposed that BCAT2 might promote the transcription of FASN and ACLY via histone acetylation. We firstly discovered that

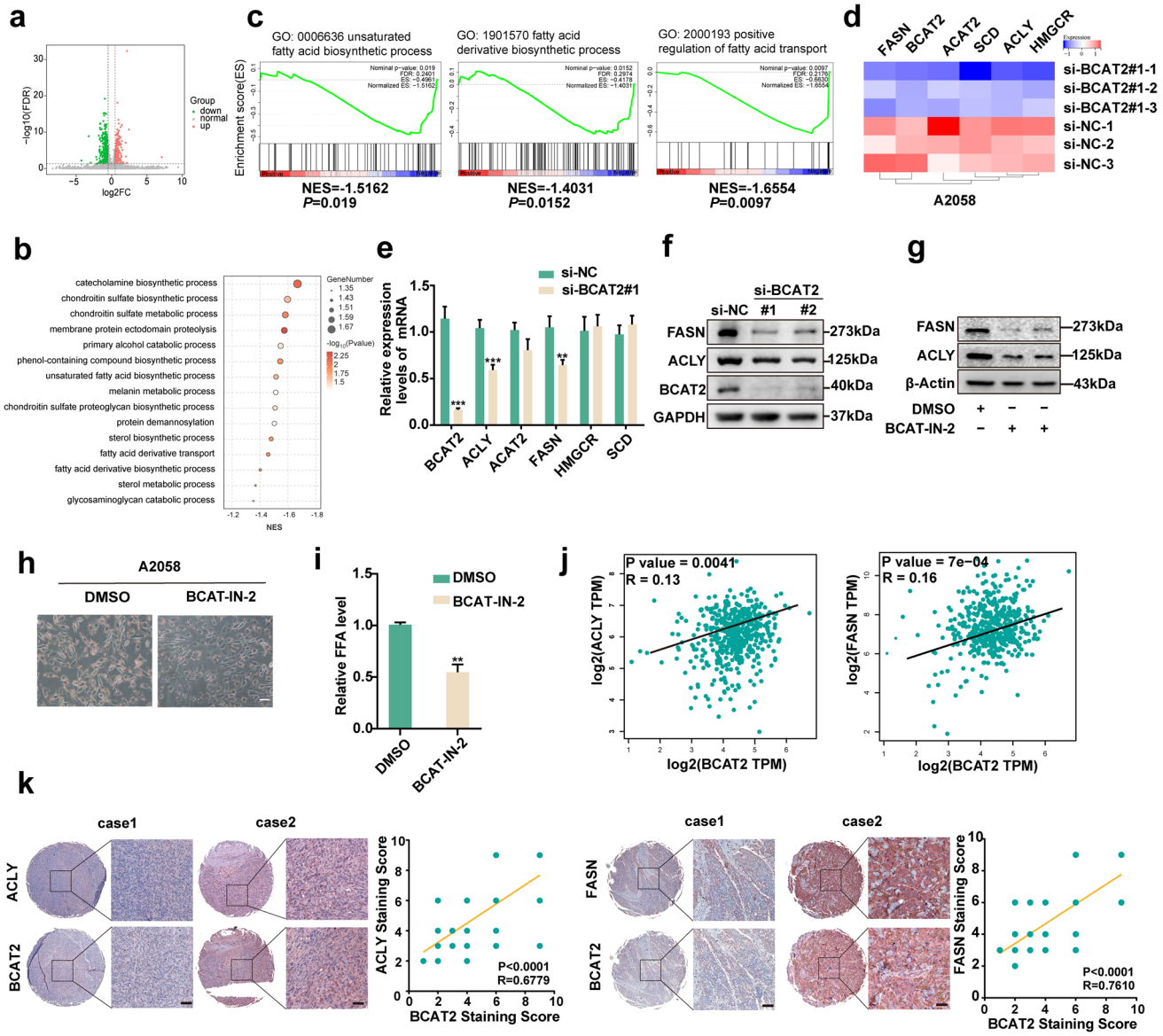

Fig. 4 BCAT2 promotes the expressions of ACLY and FASN. **a** Volcano of significantly differentially-expressed genes after BCAT2 knockdown in A2058 cell line. **b** Representative pathways enriched with differentially-expressed genes after BCAT2 knockdown in A2058 cell line. **c** GSEA analysis of differentially-expressed genes after BCAT2 knockdown in A2058 cell line. Pathways related with lipid metabolism are displayed. **d** Heatmap of representative genes significantly regulated by BCAT2 in A2058 cell line from RNA-sequencing analysis. **e** mRNA levels of key lipogenic enzymes after the knockdown of BCAT2 in A2058 cell line. **f** Immunoblotting analysis of FASN and ACLY after the knockdown of BCAT2 in A2058 cell line. **g** Immunoblotting analysis of FASN and ACLY after the pharmacological inhibition of BCAT2 (BCAT-IN-2, 80 μM). **h** Oil red staining after the inhibition of BCAT2 (BCAT-IN-2, 80 μM) in A2058 cell line. Scale bar = 100 μm. **i** Free fatty acid detection in A2058 cell line treated with BCAT2 inhibitor (BCAT-IN-2, 80 μM). **j** The correlation between BCAT2 and FASN/ACLY in TCGA SKCM database. *r* value was calculated by Spearman correlation. **k** The correlation between the staining intensities of BCAT2 and FASN/ACLY in TMA. Scale bar = 50 μm. *r* value was calculated by Spearman correlation. Data represent the mean ± SD of triplicates. *P* value was calculated by two tailed Student's t-test, $^{**}P < 0.01$, $^{***}P < 0.001$

BCAT2 inhibition led to prominent reduction of intracellular acetyl-CoA abundance, and in parallel the down-regulation of histone acetylation, in both A2058 and A375 melanoma cells (Fig. 6a and Supplementary Fig. 4a). While leucine significantly increased acetyl-CoA content and histone acetylation, concurrent inhibition of BCAT2 reversed this trend (Fig. 6b and Supplementary Fig. 4b). In addition, the supply of valine and isoleucine prominently promoted the increase of acetyl-CoA level and histone acetylation, whereas pharmacological inhibition of BCAT2 similarly suppressed this alteration (Supplementary Fig. 4c). These results demonstrated that BCAT2 is responsible for BCAA-induced

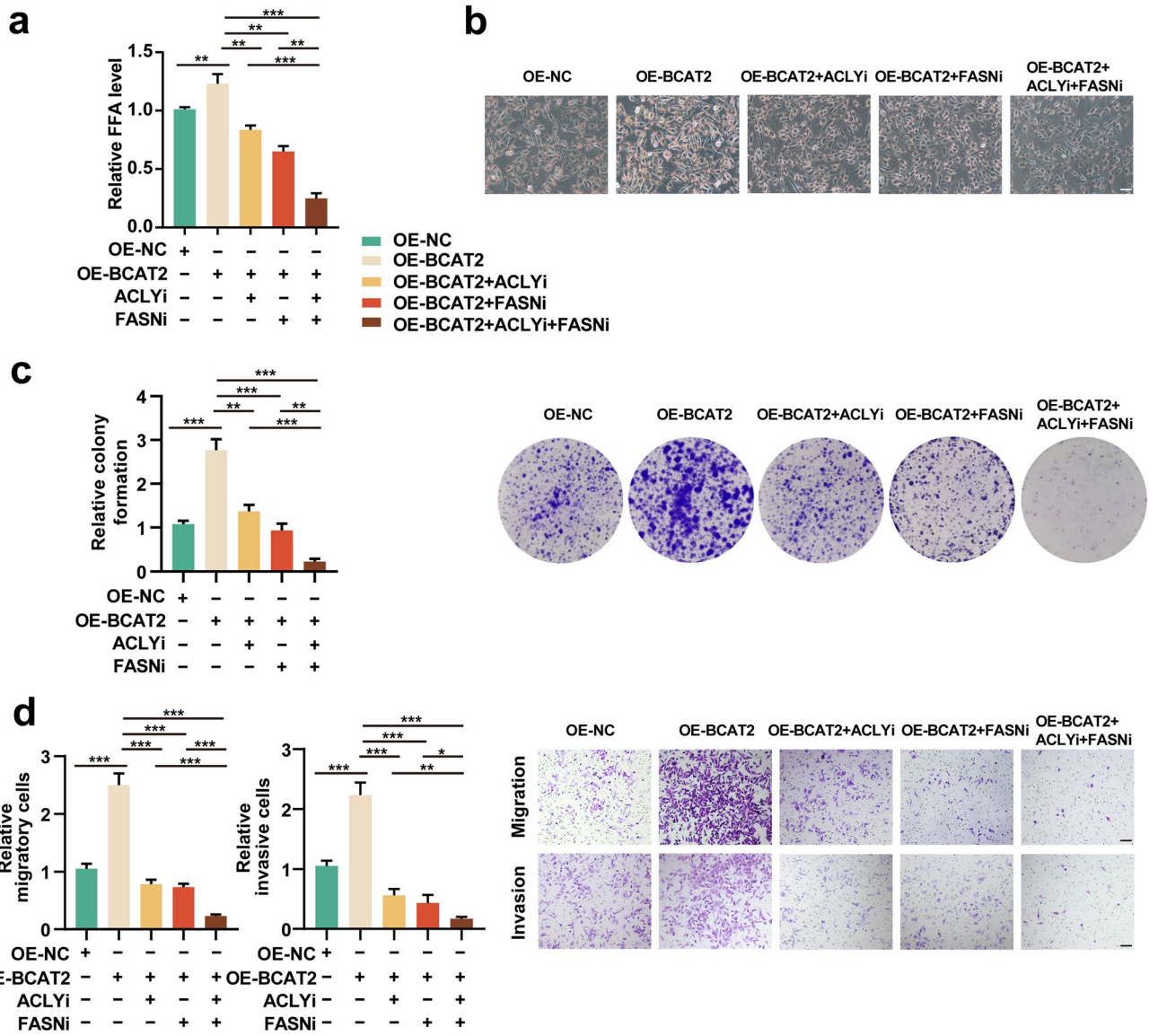

Fig. 5 BCAT2 promotes melanoma progression via the regulation of FASN and ACLY. **a** Free fatty acid detection in A2058 cell line after indicated treatment. **b** Oil red staining analysis in A2058 cell line after indicated treatment. Scale bar = 100 μm. **c** Relative colony formation of A2058 melanoma cells after indicated treatment. **d** Tumor cell migration and invasion in A2058 melanoma cells after indicated treatment (ACLYi, 20 μM, FASNi, 20 μM). Scale bar = 100 μm. Data represent the mean ± SD of triplicates. P value was calculated by two tailed Student's t-test, $^{*}P < 0.05$, $^{**}P < 0.01$, $^{***}P < 0.001$

increase of histone acetylation. What's more important, ChIP assay revealed that BCAT2 inhibition robustly reduced the enrichment of acetylated H3 on both the promoters of *FASN* and *ACLY* in both A2058 and A375 melanoma cell lines (Fig. 6c and Supplementary Fig. 4d). Moreover, the supplement of Ac-CoA by sodium acetate could reverse the down-regulation of FASN and ACLY after the pharmacological inhibition of BCAT2 (Fig. 6d and Supplementary Fig. 4e).

In addition to pharmacological intervention, we also employed genetic intervention to provide more evidence. The knockdown of BCAT2 induced the reduction of intracellular Ac-CoA level, as well as the down-regulation of histone acetylation in A2058 cell line (Supplementary Fig. 4f). Besides, BCAT2 expression deficiency abolished leucine treatment-induced increase of Ac-CoA level and histone acetylation (Supplementary Fig. 4 g). Of note, ChIP assay revealed that the knockdown of BCAT2 significantly suppressed the enrichment of acetylated H3 on both the promoters of *FASN* and *ACLY* in A2058 melanoma cell (Supplementary Fig. 4 h). The supplement of sodium acetate could also reverse the down-regulation of FASN and ACLY after

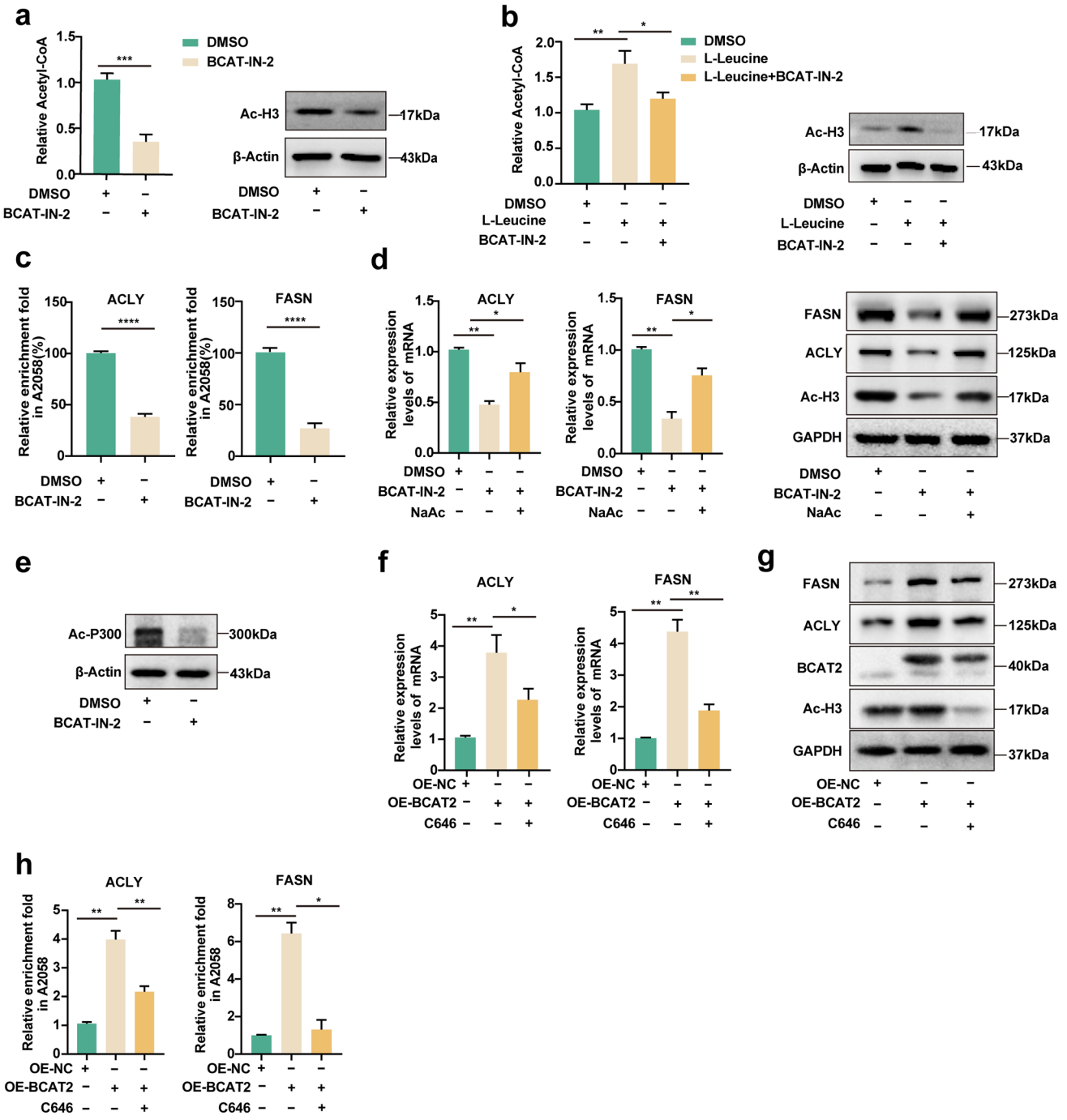

Fig. 6 P300 mediates the facilitative role of BCAT2 in promoting FASN and ACLY expressions. **a** Relative intracellular acetyl-CoA content and Ac-H3 expression after the pharmacological inhibition of BCAT2 (BCAT-IN-2, 80 μM) in A2058 melanoma cell. **b** Relative intracellular acetyl-CoA content and Ac-H3 expression in A2058 melanoma cell after the supplement with L-leucine (20 mM) and BCAT2 inhibitor (80 μM). **c** Enrichment of Ac-H3 to the promoter of *FASN* and *ACLY* after the inhibition of BCAT2 (80 μM) in melanoma. **d** mRNA and protein levels of FASN and ACLY after the treatment with BCAT2 inhibitor (80 μM) and NaAc (2.5 mM) in A2058 melanoma cell. **e** Immunoblotting analysis of acetyl-P300 after the treatment with BCAT2 inhibitor (80 μM) in A2058 melanoma cell. **f-g** mRNA and protein levels of ACLY and FASN in BCAT2-overexpressed A2058 melanoma cell with or without P300 inhibitor (C646, 10 μM). **h** Enrichment of Ac-H3 to the promoter of *FASN* and *ACLY* in BCAT2-overexpressed A2058 melanoma cell with or without P300 inhibitor (C646, 10 μM). Data represent the mean ± SD of triplicates. *P* value was calculated by two tailed Student's t-test, $^{*}P<0.05$, $^{**}P<0.01$, $^{***}P<0.001$, $^{****}P<0.0001$

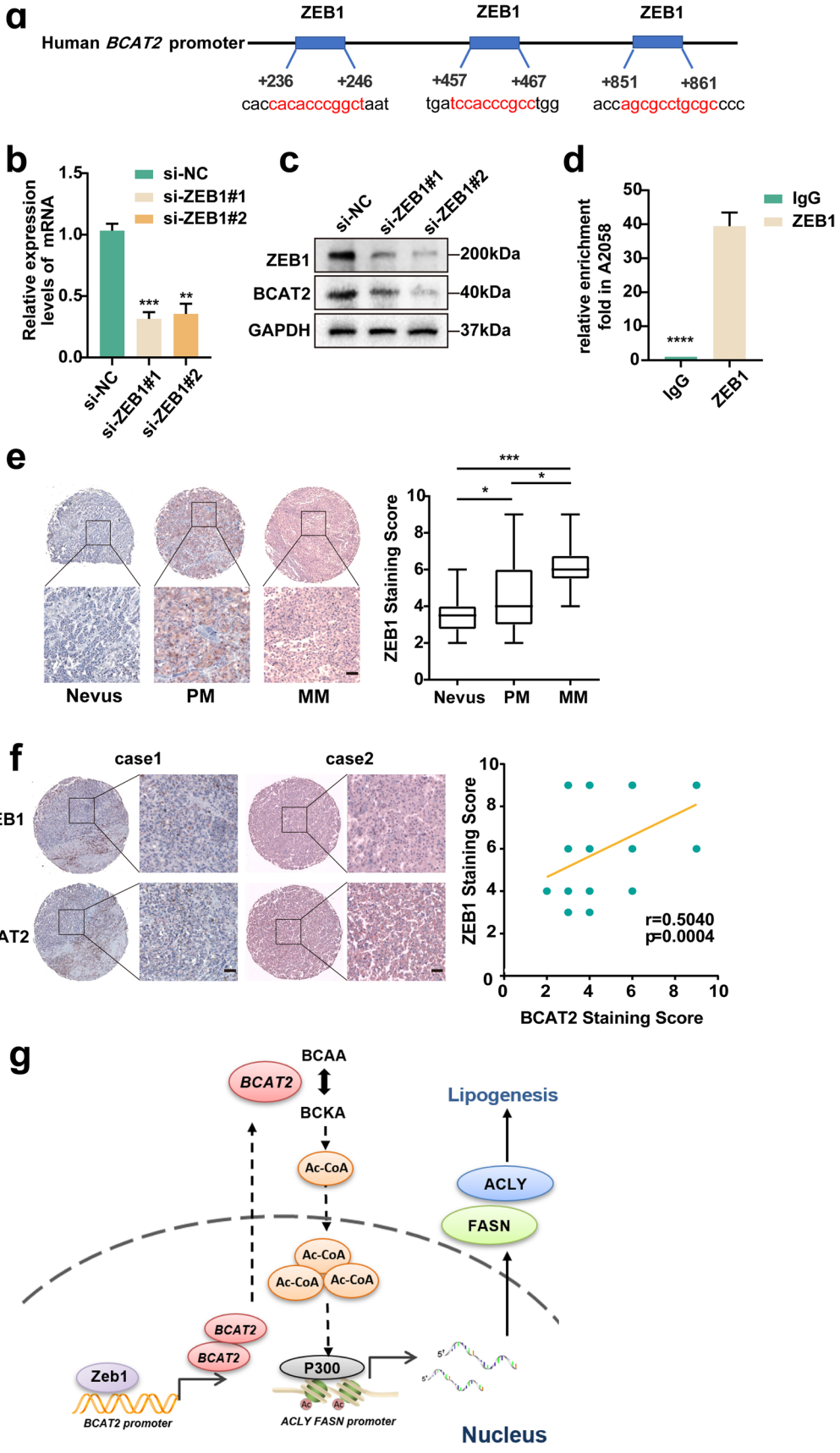
a
ZEB1
ZEB1
ZEB1
Human BCAT2 promoter
+236
+246
+457
+467
+851
+861
caccacacccggctaat
tgatccacccgcctgg
accagcgcctgcgcccc
b
Relative expression levels of mRNA
si-NC
si-ZEB1#1
si-ZEB1#2
***
**
c
si-NC
si-ZEB1#1
si-ZEB1#2
ZEB1
BCAT2
GAPDH
200kDa
40kDa
37kDa
d
relative enrichment fold in A2058
IgG
ZEB1
****
e
Nevus
PM
MM
ZEB1 Staining Score
f
case1
case2
ZEB1
BCAT2
r=0.5040
p=0.0004
BCAT2 Staining Score
g
BCAA
BCAT2
BCKA
Ac-CoA
Lipogenesis
ACLY
FASN
P300
Zeb1
BCAT2 promoter
ACLY FASN promoter
Nucleus

◂**Fig. 7** ZEB1 promotes the transcription of BCAT2 in melanoma. **a** Transcription factor analysis of *BCAT2* promoter identified three ZEB1 binding site. **b** Relative mRNA level of BCAT2 after the knockdown of ZEB1. **c** Protein level of BCAT2 after the knockdown of ZEB1. **d** Enrichment of ZEB1 to the promoter of *BCAT2* in A2058 melanoma cell. **e** The staining scores of ZEB1 in nevus and melanoma tissues. **f** Correlation between the staining scores of ZEB1 and BCAT2 in TMA. Scale bar = 50 μm. **g** A schematic model summarizing how BCAT2 promotes melanoma progression by activating lipogenesis via the epigenetic regulation of FASN and ACLY expressions. Up-regulated ZEB1 transcriptionally activates BCAT2, which promotes the generation of intracellular Ac-CoA to increase the level of histone acetylation at the promoter of both *ACLY* and *FASN* via P300. Thereafter, the transcriptional levels of ACLY and FASN are potentiated to facilitate the process of lipogenesis, ultimately leading to melanoma progression. PM, primary melanoma; MM, metastatic melanoma. Data represent the mean ± SD of triplicates. *P* value was calculated by two tailed Student's t-test, $*P < 0.05$, $***P < 0.001$, $****P < 0.0001$

the genetic knockdown of BCAT2, both in mRNA and protein levels (Supplementary Fig. 4i).

In order to provide more evidence to prove that BCAAs catabolism mediates the expressions of FASN and ACLY by altering histone acetylation in vivo, we performed ChIP-sequencing of A2058 xenografted tumors implanted in nude mice receiving BCAA dietary interventions (normal diet or high-BCAA diet). As a result, a total of 29173 peaks were identified by ChIP-sequencing in tumors in both groups (Supplementary Fig. 5a). Compared to xenografted tumors implanted in mice receiving normal diet, the binding peaks of histone acetylation to the promoter of either *FASN* and *ACLY* were higher in xenografted tumors implanted in mice receiving high-BCAA diet (Supplementary Fig. 5b). Forward ChIP assay in these xenografted tumors also confirmed that high-BCAA diet promoted more enrichment of histone acetylation on the promoter of both *ACLY* and *FASN* (Supplementary Fig. 5c), which was consistent with the result in vitro. Therefore, BCAT2 regulated FASN and ACLY expressions via altering histone acetylation.

It has been reported that the acetyltransferase activity of P300 is sensitive to the reduction of intracellular Ac-CoA content [12], and BCAT2 inhibition resulted in prominent reduction of P300 acetylation in both A2058 and A375 melanoma cell liens (Fig. 6e & Supplementary Fig. 6a), which reflected its reduced acetyltransferase activity [13]. As well, the genetic knockdown of BCAT2 also induced down-regulation of P300 acetylation in A2058 melanoma cell (Supplementary Fig. 6b). In order to see whether P300 mediated the effect of BCAT2 on FASN and ACLY expressions, melanoma cells with BCAT2 overexpression were co-treated with P300 inhibitor C646. As a result, C646 could reverse the facilitative effect BCAT2 overexpression on the mRNA levels of both FASN and ACLY (Fig. 6f and Supplementary Fig. 6c), the protein levels of histone H3 acetylation, FASN and ACLY (Fig. 6g and Supplementary Fig. 6d), and the enrichment of acetylated H3 on both the promoters of *FASN* and *ACLY* (Fig. 6h and Supplementary Fig. 6e). Therefore, P300 connected BCAT2 to histone acetylation and thereby the up-regulation of FASN and ACLY expressions.

ZEB1 is responsible for the transcriptional up-regulation of BCAT2 in melanoma

Ultimately, we went on to figure out the upstream regulatory mechanism of BCAT2. hTFtarget analysis revealed that melanoma oncogenic factor ZEB1 was among those candidate upstream regulators binding the promoter of *BCAT2* (Fig. 7a) [14]. ZEB1 is a cardinal element of a network of transcription factors that controls epithelial-to-mesenchymal transition (EMT) [15]. It has been reported that ZEB1 regulates phenotype switching toward a $MITF^{low}$ invasive and stem-like state and favors the acquisition of resistance to mitogen-activated protein kinase (MAPK)-targeted therapies in melanoma [16]. Given the crucial role of ZEB1 in melanoma pathogenesis and it might directly bind to the promoter region of *BCAT2*, we proposed that the up-regulation of oncogenic BCAT2 might be attributed to ZEB1. As a result, the knockdown of ZEB1 resulted in prominent down-regulation of BCAT2 expression in both A2058 and A375 melanoma cell lines (Fig. 7b, c and Supplementary Fig. 7a, b). ChIP assay revealed the enrichment of ZEB1 to the promoter of *BCAT2* in melanoma in both cell lines (Fig. 7d and Supplementary Fig. 7c). To rule out the off-target effect, melanoma cells with the deficiency of ZEB1 were re-overexpressed with ZEB1. The reduction of BCAT2 resulted from ZEB1 expression deficiency was rescued by ZEB1 re-overexpression (Supplementary Fig. 7d). What's more, immunohistochemical analysis in TMA showed that the staining intensity of ZEB1 was markedly higher in melanoma tissues than that in nevus tissues (Fig. 7e), and the staining intensity of BCAT2 was highly associated with that of ZEB1 (Fig. 7f). These data demonstrated that ZEB1 is responsible for the transcriptional up-regulation of BCAT2 in melanoma.

Discussion

In the present study, we firstly found that the expression of BCAT2 was prominently increased in melanoma. Then, up-regulated BCAT2 played an oncogenic role in melanoma by promoting tumor cell proliferation, invasion and migration in vitro, and tumor growth and metastasis in vivo. Subsequently, it was proved that BCAT2 regulated the expressions of FASN and ACLY to facilitate lipogenesis, resulting in tumor growth and metastasis. P300-mediated histone acetylation connected BCAT2 to transcriptional activation of FASN and ACLY. Finally, it

was documented that ZEB1 was the upstream regulator responsible for the increase of BCAT2 expression. Taken together, BCAT2 promotes melanoma progression by epigenetically regulating FASN and ACLY via P300-dependent histone acetylation (Fig. 7g). Targeting BCAT2 could be exploited as a promising strategy to restrain tumor progression in melanoma.

The pathogenic role of BCAT2 has been initially revealed in cancer. *Kras* mutation in the pancreas or the lung dictates distinct dependence on branched-chain amino acid metabolism in terms of tissue of origin. While PDAC tumors have decreased BCAA uptake, non-small cell lung carcinoma (NSCLC) tumors incorporate free BCAAs into tissue protein and use BCAAs as a nitrogen source [17]. In contrast to this, subsequent reports have revealed that BCAT2 plays an oncogenic role in PDAC progression. PDAC cells exhibit elevated BCAA uptake through solute carrier transporters, and the knockdown of BCAT2 substantially impairs PDAC cell proliferation [18]. In addition, BCAT2-mediated BCAA catabolism is critical for development of PDAC harboring *KRAS* mutations, with the enhanced mitochondrial respiration greatly implicated in [9]. Moreover, a high-BCAA diet promotes pancreatic intraepithelial neoplasia progression in mice via USP1-mediated BCAT2 stabilization [11]. Extending to the effects on cancer pathogenesis, BCAT2 is also greatly involved in the regulation of ferroptosis under the control of AMPK/SREBP1 signaling pathway [19]. Our data for the first time reports that BCAT2 acts as an oncogenic factor in melanoma by facilitating lipid metabolism. In addition to the metabolic regulation of lipogenesis via the supplement with Ac-CoA, BCAT2 could also facilitate lipogenesis via P300-dependent transcriptional up-regulation of FASN and ACLY, indicating that BCAT2 promoted lipogenesis via simultaneous metabolic and molecular regulation. In our study, we employed siRNA and shRNA transfection to obtain the knockdown of BCAT2 in melanoma cells. While the baseline expression of BCAT2 might not be that high in A2058 and A375 melanoma cells compared to other melanoma cell lines, the knockdown efficiency of BCAT2 was quite strong as the BCAT2 protein level was extremely low in si-BCAT2 group and sh-BCAT2 group. Therefore, both siRNA and shRNA worked well and there was no necessity to use CRISPR technology, let alone its expensive cost. Certainly, the limitations of using the siRNA and shRNA are off-target effect and instantaneity. To avoid the off-target effect, we performed rescue experiments via the employment of BCAT2 overexpression in melanoma cells with the knockdown of BCAT2. To solve the instantaneity of gene knockdown in the experiments in vivo, we used lentiviral vector encoding shRNAs against *BCAT2* to construct melanoma cells with BCAT2 stable knockdown. Therefore, the employment of both siRNA and shRNA could sufficiently help to prove the effect of BCAT2 in melanoma progression.

The process of de novo lipogenesis is orchestrated by a series of enzymes including ACLY, Acetyl-CoA carboxylase (ACC), FASN, Acyl-CoA Synthetase (ACS) and SCD. FASN and ACLY expressions are prominently increased in melanoma, and their high expressions are associated with a poor prognosis [12, 20]. Pharmacological inhibition of FASN by Orlistat could reduce proliferation and promote apoptosis in the mouse metastatic melanoma cell line B16-F10 [21]. Moreover, ACLY contributed to melanoma progression by enhancing mitochondrial biogenesis via MITF-PGC1α axis [12]. Previous studies have revealed some upstream regulators of FASN and ACLY. SREBP1 can transcriptionally promote the expression of FASN to mediate the process of lipogenesis [22, 23]. Moreover, FASN expression can be epigenetically regulated by histone acetylation under hypoxia to facilitate the process of lipogenesis [24]. What's more, FASN can be acetylated that can enhance its association with the E3 ubiquitin ligase TRIM21, thereby leading to decreased de novo lipogenesis and tumor cell growth [25]. In addition, ACLY can be phosphorylated by AKT or ubiquitinated by Hrd1 [26, 27]. Herein, we proved that both FASN and ACLY expressions were regulated by histone acetylation under the control of BCAT2, further supporting the crosstalk between histone acetylation-dependent epigenetics and FASN/ACLY regulation. Importantly, P300 was identified as the critical acetyltransferase responsible for the up-regulation of FASN and ACLY driven by BCAT2, highlighting that the intervention of P300 could be a useful strategy to target lipid metabolism and tumor growth in BCAT2 highly-expressed tumor. The reason for focusing on P300-dependent histone acetylation is that the up-regulation of BCAT2 promotes the generation of Ac-CoA, which plays a cardinal role in facilitating the increase of histone acetylation. Of note, a previous report has demonstrated that high-level BCAA treatment decreases the level of m^6A RNA methylation in adipose tissue and liver of weanling piglets, which might further regulate fat metabolism via the modulation of lipogenic enzymes like acetyl-CoA carboxylase (ACC) and FASN. The dysregulation of key enzymes including FTO, METTL3 and MELLT14 are responsible for decreased m^6A RNA methylation in high-BCAA group [28]. Therefore, in addition to histone acetylation, m^6A RNA methylation might also mediate the effect of BCAT2 on FASN and ACLY expressions. Whether other paradigms of epigenetic modification like methylation or SWI/SNF-dependent chromatin remodeling participates in the process of BCAT2-mediated FASN and ACLY up-regulation also needs investigations in future, though there are no reports directly demonstrating the linkage between BCAT2 and these two modes yet. In the present study, we have actually obtained the result that the inhibition of BCAT2 could induce significant down-regulation of intracellular acetyl-CoA level. The robust decrease of acetyl-CoA upon BCAT2

inhibition could be probably resulted from the following two reasons: First, the activation of BCAAs catabolism driven by BCAT2 is responsible for the generation of acetyl-CoA, so that the blockade of BCAT2 could directly induce reduction of intracellular acetyl-CoA; second, the up-regulation of ACLY induced by BCAT2 also plays a facilitative role in the generation of acetyl-CoA, so that the prominent down-regulation of acetyl-CoA after BCAT2 deficiency might also be attributed to the loss-of-function of ACLY. We would make efforts to provide more convincing evidence to figure out the reason for acetyl-CoA down-regulation after the inhibition with BCAT2 using isotopic labeling strategy in the future.

ZEB1 is a fundamental element of a network of transcription factors that controls epithelial-to-mesenchymal transition (EMT) [29]. Dysregulated expression of ZEB1 has been reported in a variety of human cancers, including melanoma [14]. Our data showed that the expression level of ZEB1 was markedly upregulated in primary and metastatic melanoma tissues than that in nevus tissues, which was consistent with previous study [14]. Apart from its canonical role in promoting EMT and tumor cell migration [30], the aberrant up-regulation of ZEB1 also rendered the treatment resistance to targeted therapy by promoting a reversible transition toward a $MITF^{low}/p75^{high}$ stem-like and tumorigenic phenotype [31]. The suppression of ZEB1 can facilitate cell differentiation and sensitize naive melanoma cells to MAPKi, as well as induce cell death in resistant cells. What's more, ZEB1 could also directly repress the secretion of T cell-attracting chemokines like CXCL10 to impair the recruitment of $CD8^+$T cell to tumor microenvironment, and the inhibition of ZEB1 synergizes with anti-PD-1 antibody therapy by promoting $CD8^+$T cell infiltration [16]. Our present study highlighted that ZEB1 could also regulate metabolic enzyme BCAT2 to exert its oncogenic role, extending the downstream regulatory network of ZEB1 in tumor biology. Since that the up-regulation of ACLY and FASN were reported to participate in rendering the resistance to targeted therapy, the role of ZEB1 in sensitizing melanoma cells to MAPKi could also be possibly attributed to BCAT2 and its-dependent ACLY and FASN regulation, which warrants forward investigation.

Several phase I or II clinical trials have been performed to testify the therapeutic potential of targeted inhibition of FASN in cancer (NCT03179904, NCT02980029, NCT04337580 and NCT02223247). The first-in-class oral FASN inhibitor TVB-2640 was of a predictable and manageable safety profile in patients with solid tumor. The disease control rate (DCR) with TVB-2640 monotherapy was 42%, and was further increased to 70% after the combination with paclitaxel [32]. While there is no clinical trial enrolling targeting ACLY in the treatment of cancer, pharmacological inhibition of ACLY in pre-clinical mice model revealed promising effect on suppressing melanoma tumor growth, improving the efficacy of melanoma MAPK-inhibition therapy, and enhancing anti-cancer immunosurveillance [12, 33]. Given that BCAT2 could simultaneously suppress ACLY and FASN expressions, further clinical trials are warranted to prove whether BCAT2 is a promising target to treat diseases involving the activation of lipogenesis pathway, especially melanoma and other types of cancers.

Supplementary Information The online version contains supplementary material available at https://doi.org/10.1007/s00018-023-04965-8.

Acknowledgements We thank the other participants of this work.

Authors' contributions CL and WG considered and designed the study. YT, JM, and HW performed the experiments. YT, JM, HW, XY, HW, and HZ conducted bioinformatics analysis and experiment data analyses. SG, YY, BZ, JD, TG and QS collected tissue specimens and clinical data. CL and WG wrote the paper. All authors read and approved the final manuscript.

Funding We thank the other participants of this work. The research leading to these results has received funding from National Natural Science Foundation of China (No. 82273182, 81902791, 82173395, 52150221), and Support Program of Young Talents in Shaanxi Province (No. 20200303, No. 2022SF-178).

Availability of data and material The data that support the findings of this study are available within the article and its supplementary materials.

Declarations

Conflict of interest All the authors declare no competing interest.

Ethical approval All animal experiments complied with ethical regulations and were approved by the Subcommittee on Research Animal Care of the Fourth Military Medical University (Xi'an, Shaanxi, China).

Consent for publication All authors reviewed the results and contributed to the fnal manuscript. All authors approved this manuscript for publication.

References

1. Lo JA, Fisher DE (2014) The melanoma revolution: from UV carcinogenesis to a new era in therapeutics. Science 346(6212):945–949. https://doi.org/10.1126/science.1253735
2. Schadendorf D, Fisher DE, Garbe C, Gershenwald JE, Grob JJ, Halpern A et al (2015) Melanoma. Nat Rev Dis Primers 1:15003. https://doi.org/10.1038/nrdp.2015.3
3. Siegel RL, Miller KD, Fuchs HE (2021) Jemal A (2021) cancer statistics. CA Cancer J Clin 71(1):7–33. https://doi.org/10.3322/caac.21654
4. Guo W, Wang H, Li C (2021) Signal pathways of melanoma and targeted therapy. Signal Transduct Target Ther 6(1):424. https://doi.org/10.1038/s41392-021-00827-6
5. Neinast M, Murashige D, Arany Z (2019) Branched chain amino acids. Annu Rev Physiol 81:139–164. https://doi.org/10.1146/annurev-physiol-020518-114455

6. Sivanand S, Vander Heiden MG (2020) Emerging roles for branched-chain amino acid metabolism in cancer. Cancer Cell 37(2):147–156. https://doi.org/10.1016/j.ccell.2019.12.011
7. Zhang B, Xu F, Wang K, Liu M, Li J, Zhao Q et al (2021) BCAT1 knockdown-mediated suppression of melanoma cell proliferation and migration is associated with reduced oxidative phosphorylation. Am J Cancer Res 11(6):2670–2683
8. Ko T, Sharma R, Li S (2020) Genome-wide screening identifies novel genes implicated in cellular sensitivity to BRAF(V600E) expression. Oncogene 39(4):723–738. https://doi.org/10.1038/s41388-019-1022-0
9. Li JT, Yin M, Wang D, Wang J, Lei MZ, Zhang Y et al (2020) BCAT2-mediated BCAA catabolism is critical for development of pancreatic ductal adenocarcinoma. Nat Cell Biol 22(2):167–174. https://doi.org/10.1038/s41556-019-0455-6
10. Lei MZ, Li XX, Zhang Y, Li JT, Zhang F, Wang YP et al (2020) Acetylation promotes BCAT2 degradation to suppress BCAA catabolism and pancreatic cancer growth. Signal Transduct Target Ther 5(1):70. https://doi.org/10.1038/s41392-020-0168-0
11. Li JT, Li KY, Su Y, Shen Y, Lei MZ, Zhang F et al (2022) Diet high in branched-chain amino acid promotes PDAC development by USP1-mediated BCAT2 stabilization. Natl Sci Rev 9(5):212. https://doi.org/10.1093/nsr/nwab212
12. Guo W, Ma J, Yang Y, Guo S, Zhang W, Zhao T et al (2020) ATP-Citrate lyase epigenetically potentiates oxidative phosphorylation to promote melanoma growth and adaptive resistance to MAPK inhibition. Clin Cancer Res 26(11):2725–2739. https://doi.org/10.1158/1078-0432.CCR-19-1359
13. Marino G, Pietrocola F, Eisenberg T, Kong Y, Malik SA, Andryushkova A et al (2014) Regulation of autophagy by cytosolic acetyl-coenzyme A. Mol Cell 53(5):710–725. https://doi.org/10.1016/j.molcel.2014.01.016
14. Denecker G, Vandamme N, Akay O, Koludrovic D, Taminau J, Lemeire K et al (2014) Identification of a ZEB2-MITF-ZEB1 transcriptional network that controls melanogenesis and melanoma progression. Cell Death Differ 21(8):1250–1261. https://doi.org/10.1038/cdd.2014.44
15. Mohammadi Ghahhari N, Sznurkowska MK, Hulo N, Bernasconi L, Aceto N, Picard D (2022) Cooperative interaction between ERalpha and the EMT-inducer ZEB1 reprograms breast cancer cells for bone metastasis. Nat Commun 13(1):2104. https://doi.org/10.1038/s41467-022-29723-5
16. Plaschka M, Benboubker V, Grimont M, Berthet J, Tonon L, Lopez J et al (2022) ZEB1 transcription factor promotes immune escape in melanoma. J Immunother Cancer. https://doi.org/10.1136/jitc-2021-003484
17. Mayers JR, Torrence ME, Danai LV, Papagiannakopoulos T, Davidson SM, Bauer MR et al (2016) Tissue of origin dictates branched-chain amino acid metabolism in mutant Kras-driven cancers. Science 353(6304):1161–1165. https://doi.org/10.1126/science.aaf5171
18. Lee JH, Cho YR, Kim JH, Kim J, Nam HY, Kim SW et al (2019) Branched-chain amino acids sustain pancreatic cancer growth by regulating lipid metabolism. Exp Mol Med 51(11):1–11. https://doi.org/10.1038/s12276-019-0350-z
19. Wang K, Zhang Z, Tsai HI, Liu Y, Gao J, Wang M et al (2021) Branched-chain amino acid aminotransferase 2 regulates ferroptotic cell death in cancer cells. Cell Death Differ 28(4):1222–1236. https://doi.org/10.1038/s41418-020-00644-4
20. Rosolen D, Kretzer IF, Winter E, Noldin VF, Rodrigues do Carmo IA, Filippin-Monteiro FB, et al (2016) N-phenylmaleimides affect adipogenesis and present antitumor activity through reduction of FASN expression. Chem Biol Interact 258:10–20. https://doi.org/10.1016/j.cbi.2016.08.005
21. Carvalho MA, Zecchin KG, Seguin F, Bastos DC, Agostini M, Rangel AL et al (2008) Fatty acid synthase inhibition with Orlistat promotes apoptosis and reduces cell growth and lymph node metastasis in a mouse melanoma model. Int J Cancer 123(11):2557–2565. https://doi.org/10.1002/ijc.23835
22. Deng J, Peng M, Zhou S, Xiao D, Hu X, Xu S et al (2021) Metformin targets Clusterin to control lipogenesis and inhibit the growth of bladder cancer cells through SREBP-1c/FASN axis. Signal Transduct Target Ther 6(1):98. https://doi.org/10.1038/s41392-021-00493-8
23. Husain A, Chiu YT, Sze KM, Ho DW, Tsui YM, Suarez EMS et al (2022) Ephrin-A3/EphA2 axis regulates cellular metabolic plasticity to enhance cancer stemness in hypoxic hepatocellular carcinoma. J Hepatol 77(2):383–396. https://doi.org/10.1016/j.jhep.2022.02.018
24. Gao X, Lin SH, Ren F, Li JT, Chen JJ, Yao CB et al (2016) Acetate functions as an epigenetic metabolite to promote lipid synthesis under hypoxia. Nat Commun 7:11960. https://doi.org/10.1038/ncomms11960
25. Lin HP, Cheng ZL, He RY, Song L, Tian MX, Zhou LS et al (2016) Destabilization of fatty acid synthase by acetylation inhibits de novo lipogenesis and tumor cell growth. Cancer Res 76(23):6924–6936. https://doi.org/10.1158/0008-5472.CAN-16-1597
26. Martinez Calejman C, Trefely S, Entwisle SW, Luciano A, Jung SM, Hsiao W et al (2020) mTORC2-AKT signaling to ATP-citrate lyase drives brown adipogenesis and de novo lipogenesis. Nat Commun 11(1):575. https://doi.org/10.1038/s41467-020-14430-w
27. Li K, Zhang K, Wang H, Wu Y, Chen N, Chen J et al (2021) Hrd1-mediated ACLY ubiquitination alleviate NAFLD in db/db mice. Metabolism 114:154349. https://doi.org/10.1016/j.metabol.2020.154349
28. Heng J, Wu Z, Tian M, Chen J, Song H, Chen F et al (2020) Excessive BCAA regulates fat metabolism partially through the modification of m(6)A RNA methylation in weanling piglets. Nutr Metab (Lond) 17:10. https://doi.org/10.1186/s12986-019-0424-x
29. Caramel J, Ligier M, Puisieux A (2018) Pleiotropic Roles for ZEB1 in Cancer. Cancer Res 78(1):30–35. https://doi.org/10.1158/0008-5472.CAN-17-2476
30. Wels C, Joshi S, Koefinger P, Bergler H, Schaider H (2011) Transcriptional activation of ZEB1 by Slug leads to cooperative regulation of the epithelial-mesenchymal transition-like phenotype in melanoma. J Invest Dermatol 131(9):1877–1885. https://doi.org/10.1038/jid.2011.142
31. Richard G, Dalle S, Monet MA, Ligier M, Boespflug A, Pommier RM et al (2016) ZEB1-mediated melanoma cell plasticity enhances resistance to MAPK inhibitors. EMBO Mol Med 8(10):1143–1161. https://doi.org/10.1525/emmm.201505971
32. Falchook G, Infante J, Arkenau HT, Patel MR, Dean E, Borazanci E et al (2021) First-in-human study of the safety, pharmacokinetics, and pharmacodynamics of first-in-class fatty acid synthase inhibitor TVB-2640 alone and with a taxane in advanced tumors. EClinicalMedicine 34:100797. https://doi.org/10.1016/j.eclinm.2021.100797
33. Pietrocola F, Pol J, Vacchelli E, Rao S, Enot DP, Baracco EE et al (2016) Caloric restriction mimetics enhance anticancer immunosurveillance. Cancer Cell 30(1):147–160. https://doi.org/10.1016/j.ccell.2016.05.016